

Aalborg Universitet



Robust Solar Position Sensor for Tracking Systems

Ritchie, Ewen; Argeseanu, Alin; Leban, Krisztina Monika

Published in:
Proceedings of 9th WSEAS International Conference on Power Systems (PS' 09)

Publication date:
2009

Document Version
Publisher's PDF, also known as Version of record

[Link to publication from Aalborg University](#)

Citation for published version (APA):
Ritchie, E., Argeseanu, A., & Leban, K. M. (2009). Robust Solar Position Sensor for Tracking Systems. In *Proceedings of 9th WSEAS International Conference on Power Systems (PS' 09)* (pp. 49-54). WSEAS Press.

General rights

Copyright and moral rights for the publications made accessible in the public portal are retained by the authors and/or other copyright owners and it is a condition of accessing publications that users recognise and abide by the legal requirements associated with these rights.

- Users may download and print one copy of any publication from the public portal for the purpose of private study or research.
- You may not further distribute the material or use it for any profit-making activity or commercial gain
- You may freely distribute the URL identifying the publication in the public portal -

Take down policy

If you believe that this document breaches copyright please contact us at vbn@aub.aau.dk providing details, and we will remove access to the work immediately and investigate your claim.

Robust Solar Position Sensor for Tracking Systems

EWEN RITCHIE

Department of Energy Technology
University of Aalborg
Pontoppidanstræde 101, DK-9220, Aalborg
Denmark
aer@iet.aau.dk <http://www.iet.aau.dk/~aer>

ALIN ARGESSEANU

Electrical Engineering, MAUE
University Politehnica Timisoara
Bl. Vasile Parvan no.2, Timisoara
ROMANIA
alin.argeseanut@et.upt.ro

KRISZTINA LEBAN

Department of Energy Technology
University of Aalborg
Pontoppidanstræde 101, DK-9220, Aalborg
Denmark
krisztina_leban@yahoo.com.au <http://www.iet.aau.dk>

Abstract: - The paper proposes a new solar position sensor used in tracking system control. The main advantages of the new solution are the robustness and the economical aspect. Positioning accuracy of the tracking system that uses the new sensor is better than 1° . The new sensor uses the ancient principle of the solar clock. The sensitive elements are eight ordinary photo-resistors. It is important to note that all the sensors are not selected simultaneously. It is not necessary for sensor operating characteristics to be quasi-identical because the sensor principle is based on extreme operating duty measurement (bright or dark). In addition, the proposed solar sensor significantly simplifies the operation of the tracking control device.

Key-Words: - solar energy, tracking systems, optimum-optimum receiver position, photo-resistors, matrix sensor, digital code converter, digital comparator.

1 Introduction

Renewable energy is a key concept in the 21st century. The catastrophic climate change, increasing energy needs in emerging economies (China, India), exhaustion of the classical energy resources and a secure energy supply are the principal features that must be taken into account when attempting to present the future of the world in an optimistic vision. The man-made changes of concentration of carbon-dioxide, methane and nitrous oxide are the principal factors that motivate interest in increasing renewable energy production. The main topics include photovoltaic, solar thermal energy, geothermal energy, wind energy, wave energy, bio-energy, hydrogen technologies and solar-assisted cooling systems. Renewable energy involves efficient energy collection, efficient storage and

transport and efficient energy conversion. To achieve an efficient solar energy capture imposes three important requirements: concentrators, tracking systems and MPP (Maximum Power Point) trackers. Simultaneous goals of the solar energy systems design are the robustness of the equipments and the cost of produced energy. The real and expected growth of solar (photovoltaic and thermal) energy has already applied some pressure on the supply of the most specialized types of motion components. Suppliers of drive systems and mechanical components have reported a huge upswing in interest from OEMs who integrate solar power systems with Sun-tracking capabilities, because the positioning accuracy of a solar tracking system improves the energy collection of the whole system.

The double movement of the Earth, around the Sun and the rotation about its inclined polar axis is shown in Fig.1.

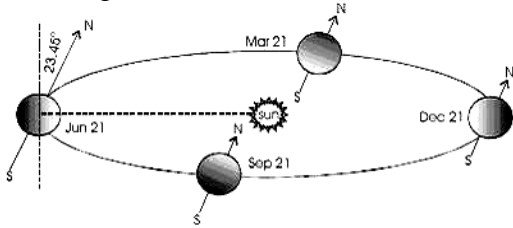


Fig.1. The Earth's orbit around the Sun, showing the inclined axis of diurnal rotation

The angle of deviation of the Sun from directly above the equator is the declination angle, δ . The mathematical expression of the declination in accord with the day (n) of the year is [1]:

$$\delta = 23.45^\circ \cdot \sin\left[\frac{360 \cdot (n-180)}{365}\right] \quad (1)$$

In (1), those angles north of the equator are positive and those south of the equator are negative.

The zenith angle, ϑ_z , is the angle between the Sun and a line perpendicular to the Earth's surface (the zenith line). Since the Sun is directly overhead on the first day of summer, at noon, on the tropic of cancer, the zenith angle is given by:

$$\vartheta_z = \phi - \delta \quad (2)$$

where ϕ = the latitude in degrees

The relations between the deviation angle and the zenith angle are illustrated in Fig.2.

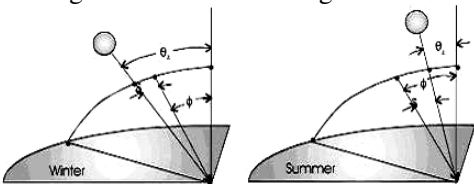


Fig.2. The relation between deviation and zenith angles

If we assume the distance from the Earth to the Sun to be constant, the position of the Sun can be completely specified by two coordinates: the solar altitude and the azimuth. The solar altitude α , is the complement of the zenith angle ϑ_z . The solar altitude represents the angle between the incident solar beam and the horizon, in the plane determined by the Sun and the zenith. The necessary pair of coordinates is illustrated in Fig.3. The angle ψ is the azimuth angle and measures the angular deviation of the Sun from due south. The azimuth angle is zero at solar noon and increases toward the

east. In some papers, the azimuth angle is referenced to north and in this case the solar noon appears at $\psi = 180^\circ$. The angle ω describes the angular displacement of the Sun from solar noon in the plane of apparent travel of the Sun. This angle is useful but redundant in the system of solar coordinates.

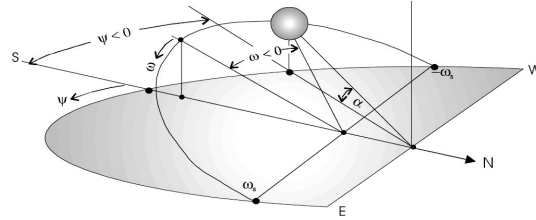


Fig.3. Illustrating the pair of coordinates necessary in a complete determination of the solar position

The relationships between ψ and α may be determined, but are difficult to visualize. For this reason it is convenient to plot the values of angles ψ and α for specific latitudes and days of the year. Fig.4 shows a set of plots for the case of a latitude $30^\circ N$ [2]

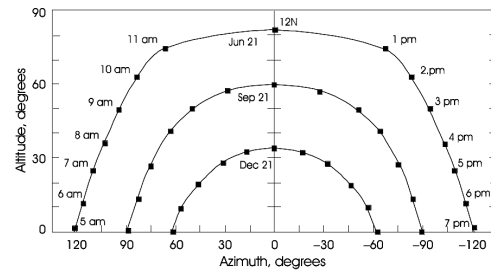


Fig.4. The values of angles ψ and α for a latitude of $30^\circ N$

Irradiance is the measure of the power density of Sunlight. Is an instantaneous quantity and is measured in W/m^2 . The irradiance received by the Earth from the Sun at the top of the atmosphere is constant, equal to $1367 W/m^2$. The irradiance is reduced after passing through the atmosphere to an approximate value of $1000 W/m^2$. The direct normal solar irradiance is given by:

$$I_{t,h} = I_{b,n} \cdot \cos \vartheta_z + I_{d,h} \quad (3)$$

$I_{b,n}$ = the irradiance coming directly from the Sun

$I_{d,n}$ = the diffuse radiation

The clear-day model of direct normal solar irradiance using the U.S. Standard Atmosphere (Hottel model) is given by [3][4]:

$$I_{b,n} = I_0 \left(a_0 + a_1 e^{-k \frac{1}{\cos \theta_z}} \right) \quad (4)$$

I_0 = the extraterrestrial radiation

a_0, a_1, k = parameters

More solar energy is collected by the end of the day if the solar receivers (photovoltaic or thermal) are installed with a tracker system. For a planar receiver, the receiver plane must be perpendicular to the direction of the solar flux irradiance. The solar energy collected is proportional to the cosine of the angle between the incident beam and the normal of the plane of the collector, as shown in Fig.5. [4]

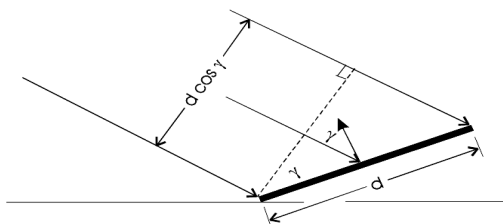


Fig.5. The collected solar energy

There are two types of Sun trackers:

- A one-axis tracker: follows the Sun from east to west during the day
- A two-axis tracker: maintains the receiver surface perpendicular to the Sun and allows collection of the maximum possible amount of energy.

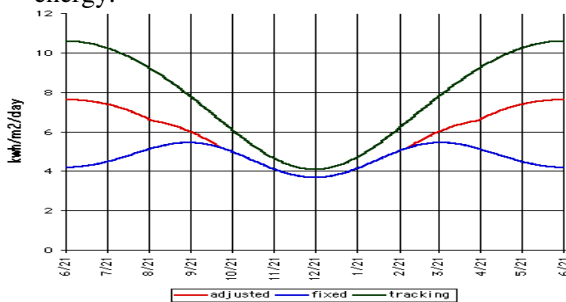


Fig.6. The collected energy by fixed and tracker receivers

The collected Sun energy improves by 40%-50% using tracking systems (35%-42% by E-W tracker and 5%-8% by N-S tracker). The improvement in the collected energy varies during the year. The energy collected for a fixed receiver, an adjusted one (one axis) and a two-axis tracker is depicted in Fig.6. In the summer time and in a dry climate, the additional energy is approximately 50% but in the winter time, the additional energy is only 20%.

2 Sun tracker control systems

Sun tracker control systems use two major strategies:

- the sensor control: the Sun's position is specified using two coordinates and the optimum-optimum position is estimated using photosensors signals.

- the sensorless control: the optimum-optimum values of the Sun coordinates are calculated for the any moment of the day, during all year, in the case of a fixed location of the solar collector. Using this data base, the tracking system moves the collector to the optimum-optimum position. The data base must be calculated for every geographical location of the Sun collector.

The Sun tracking controllers were developed following the classical control system closed-loop approach by integrating a Sun sensor able to provide pointing-error signals, one per tracking axis. This in turn generates actuator correction movements. Each Sun sensor comprises a pair of phototransistors, generate different photocurrents whenever the sensor is not aligned with the local Sun vector. The phototransistors may be mounted on tilted planes in order to increase sensitivity. In some applications, the shading devices are provided. Some types of Sun sensor are shown in Fig.7.[5]

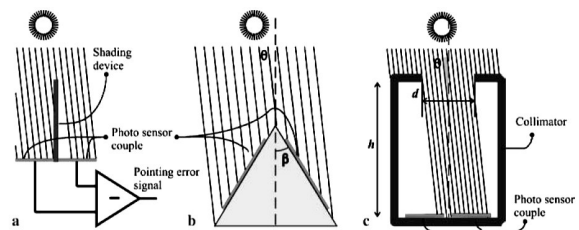


Fig.7. Various types of Sun sensor

A classical sensor for one Sun position coordinate uses a pair of phototransistors mounted on titled planes. The angle of tilt of the plane is 90^0 . The device is encased to provide protection. The construction of the sensor is illustrated in Fig.8.

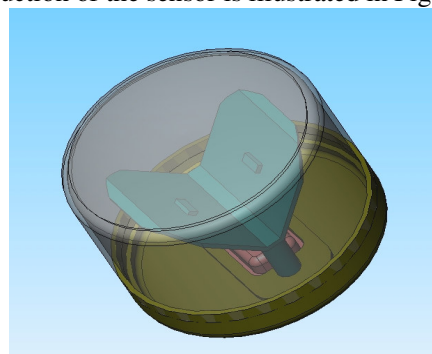


Fig.8 A classical Sun sensor

There are two important problems: for each sensor the phototransistors must be quasi-identically, because the measurement method assumes identically currents in the case of identically irradiance. If the characteristics of the phototransistors are not identically, the position of the collector is not the optimal position. The second

problem is the ageing semiconductor effect. The ageing phototransistors effects and the accidentally greasing of the sensor box induce a faulty function of the tracking system.

2.1 Proposed new Sun sensor design

The problems of the classical Sun sensor may be solved by the proposed new type of matrix Sun sensor (MSS). In the previous solutions, each tracking direction is controlled by using a Sun sensor made by a pair of phototransistors. This proposal is for a single matrix Sun sensor MSS which controls both axes of the tracking system. The inspiration for the MSS is the antique solar clock. MSS comprises 8 photo-resistors and a cylinder. The location of the cylinder is at the centre of the matrix structure of the photo-resistors, which are evenly distributed around a circle. If the position of the collector is not optimum, the shadow of the cylinder covers one or two photo-resistors. The photo-resistors are mounted circular, around the cylinder, as shown in Fig.9:

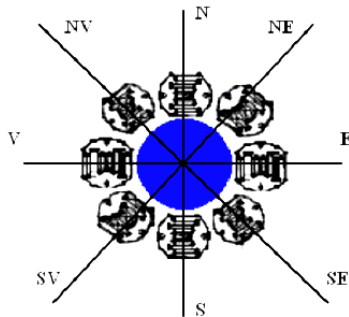


Fig.9 The photoresistors matrix

The photo-resistor is a high resistance semiconductor whose resistance decreases with increasing intensity of incident light. It is a light dependent resistor device. The cadmium sulphide cell, CdS cell, is the most inexpensive type of photo-resistor (the price of a CdS cell is 10-12 eurocents). This is why the proposed implementation of MSS uses CdS cells. There are two important observations about MSS operation:

- the classical control system closed-loop approach is substituted by a simple digital circuit
- the MSS works in a digital kind of way: each CdS cell has two states, illuminated state and shaded state

2.1.1 MSS sizing and additionally circuits

The topology and working principle of the proposed MSS respect the antique solar clock. Each CdS cell corresponds to a direction: N, NE, E, SE, S, SW, W and NW (see Fig.9). The MSS logic operation is:

- if the N CdS cell is shaded, the N-S actuator moves in the opposite direction, southward.
- if the N-E CdS cell is shaded, both actuators must move in the opposite direction: N-S actuator moves southward and E-V actuator moves westward.
- if the E CdS cell is shaded, the E-V actuator moves in the opposite direction, westward.
- if the S-E CdS cell is shaded, both actuators must move in the opposite direction: N-S actuator moves northward and E-V actuator moves westward.
- if the S CdS cell is shaded, the N-S actuator moves in the opposite direction, northward.
- -if S-W CdS cell is shaded, both actuators must move in the opposite direction: N-S actuator moves northward and E-V actuator moves eastward
- if the W CdS cell is shaded, the E-V actuator moves in the opposite direction, eastward.
- if the N-W CdS cell is shaded, both actuators must move in the opposite direction: N-S actuator moves southward and E-V actuator moves eastward.

The difference between a shaded CdS cell and a lighted CsS cell is recognised using the current values of the cell resistance. The electronic circuit is a simple, robust, low-cost voltage divider circuit. Two circuit variants are illustrated in Fig.10:

- the output voltage increases when the irradiance increases (Fig.10 a)
- the output voltage decreases when the irradiance increases (Fig.10 b)

For the a,b circuits, the output voltages are:

$$V_{out} = \frac{R_2}{R_2 + R_1} \cdot V_{cc} \tag{5}$$

$$V_{out} = \frac{R_1}{R_2 + R_1} \cdot V_{cc} \tag{6}$$

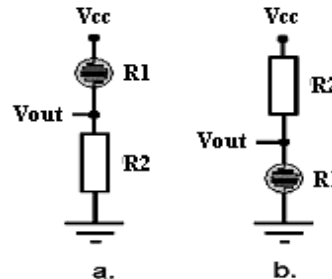


Fig.10 Voltage divisor circuits for CdS cell

The MSS uses the divider circuit type a.

The resistance R_2 is: $R_2 = \sqrt{R_{ldark} \cdot R_{lbright}}$. It is necessary to measure the resistance of all CdS cells

with respect to the level of illumination. The values are in the Table 1. The percentages represent the levels of lighted area of a cell.

	N	NW	W	SW	S	SE	E	NE
100%	46.4	40.6	42.8	41.4	39.4	40.4	41.8	42
75%	62.8	55	61.6	54.6	50.2	53	57.4	56.6
50%	78.4	78.2	77	65.6	67.4	70.2	73.4	80.6
25%	110.4	101.8	116.6	99.4	110.6	112.2	112.6	110
0%	263	171.2	205.2	186.6	234.2	254	293	307.6

Table 1. The values of CdS cell resistance

Using the relationship for R_2 , the computed values are in Table 2:

	N	NW	W	SW	S	SE	E	NE
R_2	110.5	83.4	93.7	87.9	96	101.3	110.7	113.7

Table 2. The values of computed R_2

For the same condition of illumination the values of the CdS cell resistances are different, according to their position relative to the central cylinder. The variations are important. The classical Sun position sensor cannot work under these conditions. The variations referred to the mean values are shown in Table 3.

	$\epsilon\%$ N	$\epsilon\%$ NE	$\epsilon\%$ E	$\epsilon\%$ SE	$\epsilon\%$ S	$\epsilon\%$ SW	$\epsilon\%$ W	$\epsilon\%$ NW
100%	10.9	-2.9	2.3	1.1	-5.8	-3.4	-0.1	0.4
75%	11.3	-2.5	9.2	-3.2	-11	-6	1.8	0.3
50%	6.1	5.8	4.2	-11.2	-8.8	-5	-0.7	9
25%	1.1	-6.8	6.8	-8.9	1.3	2.7	3.4	0.7
0%	9.9	-28.5	-14.2	-22	-2.1	6.1	22.4	28.5

Table 3. The errors of CdS cells resistances

Using data from Table 2, the value of R_2 is 120 Ω . The output voltages, in accord with relationship (5), using the value of $R_2=120 \Omega$, the reference voltage $V_{CC}=5V$ and the measured resistances of the CdS cells from Table 1, are presented in Table 4 (all values are given in V).

	U_N	U_{NE}	U_E	U_{SE}	U_S	U_{SW}	U_W	U_{NW}
100%	3.60	3.73	3.68	3.71	3.78	3.74	3.70	3.71
75%	3.28	3.42	3.30	3.43	3.52	3.46	3.38	3.39
50%	3.02	3.02	3.04	3.23	3.20	3.15	3.10	2.99
25%	2.60	2.70	2.53	2.73	2.60	2.58	2.57	2.60
0%	1.56	2.06	1.84	1.95	1.69	1.60	1.45	1.40

Table 4. The output voltages of CdS divisor circuits

The voltage variations of all CdS circuits, for the same illumination conditions are given in Table 5. The variations are reduced (the effect of the presence of R_2) but there are still significant.

	$\epsilon\%$ N	$\epsilon\%$ NE	$\epsilon\%$ E	$\epsilon\%$ SE	$\epsilon\%$ S	$\epsilon\%$ SW	$\epsilon\%$ W	$\epsilon\%$ NW
100%	-2.9	0.5	-0.1	0	1.9	0.8	-0.2	0
75%	-3.5	0.6	-2.9	0.9	3.5	1.8	-0.6	-0.3
50%	-2.5	-2.5	-1.9	4.2	3.2	1.6	0	-3.5
25%	0	3.8	-2.7	5	0	-0.8	-1.1	0
0%	-8.2	21	8.2	14.7	-0.6	-5.9	-14	-17

Table 5. Voltage variations of the CdS divisor circuits

It is possible to obtain Sun sensor accuracy smaller than 1° if MSS uses a “binary” technique: MSS compares illuminated CdS cells with shaded CdS cells. This operation is performed using eight comparator circuits. Each comparator uses 2 signals: the output voltage of the divider circuits and the reference voltage. The reference voltage is selected in the illumination range 0%-30%, from Table 4. If the selected reference voltage is 2V-2.5V, MSS and the comparators block generate a binary output: 1 if the CdS cell is lighted and 0 if the CdS cell is shaded. The output signals of the comparator block are: N, NE, E, SE, S, SW, W, NW.

The MSS discrimination is defined by the dimensions of the central cylinder. If the accuracy is fixed 1° , the length of the cylinder may be determined by a simple trigonometric relationship, as shown in Fig.11. When the deviation of the optimum position of the collector is 1° , the shadow of the cylinder cast must be 3mm (the dimension of the CdS cell). The length of the cylinder is thus:

$$h = \frac{s}{\tan \alpha} = \frac{3}{\tan 1^\circ} \approx 17 [cm] \tag{7}$$

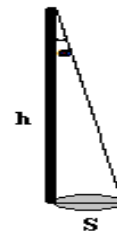


Fig.11. Cylinder sizing

2.1.2 MSS digital control

The binary character of the new MSS suggests a simple digital control of the tracker actuators. Circuit design starts with the truth table, see Table 6, where the input signals are N, NE, E, SE, S, SW,

W, and NW (these signals are the output digital set of the comparator block) and the output signals, D_N , D_E , D_S , D_W , determine the start/stop functions of the N-S and E-W actuators.

N	NE	E	SE	S	SW	W	NW	D_N	D_E	D_S	D_W
1	0	0	0	0	0	0	0	0	0	1	0
1	1	0	0	0	0	0	0	0	0	1	1
0	1	0	0	0	0	0	0	0	0	1	1
0	1	1	0	0	0	0	0	0	0	1	1
0	0	1	0	0	0	0	0	0	0	0	1
0	0	1	1	0	0	0	0	1	0	0	1
0	0	0	1	0	0	0	0	1	0	0	1
0	0	0	1	1	0	0	0	1	0	0	1
0	0	0	0	1	0	0	0	1	0	0	0
0	0	0	0	1	1	0	0	1	1	0	0
0	0	0	0	0	1	0	0	1	1	0	0
0	0	0	0	0	1	1	0	1	1	0	0
0	0	0	0	0	0	1	0	0	1	0	0
0	0	0	0	0	0	1	1	0	1	1	0
0	0	0	0	0	0	0	1	1	0	1	0
1	0	0	0	0	0	0	1	0	1	1	0

Table 6. The truth table of the digital MSS device

For other combinations all outputs become zero. The shaded values are redundant. The optimized truth table is given in Table 7:

N	NE	E	SE	S	SW	W	NW	D_N	D_E	D_S	D_W
1	0	0	0	0	0	0	0	0	0	1	0
0	1	0	0	0	0	0	0	0	0	1	1
0	0	1	0	0	0	0	0	0	0	0	1
0	0	0	1	0	0	0	0	1	0	0	1
0	0	0	0	1	0	0	0	1	0	0	0
0	0	0	0	0	1	0	0	1	1	0	0
0	0	0	0	0	0	1	0	0	1	0	0
0	0	0	0	0	0	0	1	0	1	1	0

Table 7 The optimized truth table

The output signals are:

$$D_N = SE + S + SW, \quad D_E = SW + W + NW, \\ D_S = NE + N + NW, \quad D_W = NE + E + SE, \quad (8)$$

Practically, there are some forbidden input signals combinations. The shadow area can cover one, maximum two adjacent areas. The correct combinations are: N-NE, NE-E, E-SE, SE-S, S-SW, SW-W, W-NW, NW-W. All these combinations are in the digital relationships (8). The forbidden combinations are: N-E, N-SE, N-S, N-SW, N-W, NE-SE, NE-S, NE-SW, NE-W, NE-NW, E-S, E-SW, E-W, E-NW, SE-SW, SE-W, SE-NW, S-W, S-SW, SW-NW. The digital circuit is a code convert type and is illustrated in Fig.12. The new MSS was tested in a solar parabolic dish thermal collector, at Politehnica University Timisoara, Romania (Fig.13).

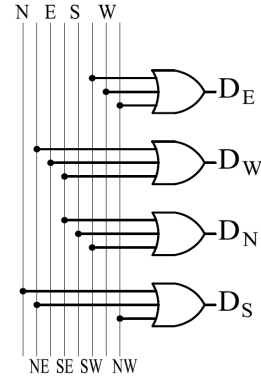


Fig.12. Code converter circuit



Fig.13. A solar parabolic dish thermal collector using the new MSS

3 Conclusion

A new Sun sensor matrix structure is proposed. MSS uses low cost unsorted photoelements (CdS cells). CdS cell works in a digital way because MSS observe 2 extreme situations: lighted and shaded CdS cell resistances. The MSS discrimination is better than 1° and it is constructed using a cylinder mounted in the centre of the CdS matrix structure. The sensor is robust, low cost and determines a simple digital control of the actuators of the Sun tracker.

References:

- [1] A Luque Handbook of Photovoltaic Science and Engineering, John Wiley&Sons, 2003
- [2] A Messenger, J Ventre, Photovoltaic System Engineering, CRC Press, 2003
- [3] A Goetzberger, V Hoffmann, Photovoltaic Solar Energy Generation, Springer, 2005
- [4] M R Patel, Wind and Solar Power System, CRC Press, 1999
- [5] A Luque, VM Andreev, Concentrator Photovoltaics, Springer, 2007